Available online at www.sciencedirect.com
SCIENCE DIRECT
Journal of Solid State Chemistry 179 (2006) 855–865
JOURNAL OF SOLID STATE CHEMISTRY
www.elsevier.com/locate/jssc

# MFI-type boroaluminosilicate: A comparative study between the direct synthesis and the templating method

Wei Zhou, Shi-Yu Zhang, Xiang-Ying Hao, Hao Guo, Cui Zhang, Yin-Qing Zhang, Shuangxi Liu*

*Institute of New Catalytic Materials Science, College of Chemistry, Nankai University, Tianjin 300071, People's Republic of China*

Received 24 October 2005; received in revised form 8 December 2005; accepted 10 December 2005
Available online 24 January 2006

**Abstract**

Boroaluminosilicate with MFI zeotype (henceforth B-ZSM-5) was synthesized both via the direct synthesis where ZSM-5 was employed as crystal seed and the templating method by using TPABr as the structure-directing agent (SDA). Characterization based on its structure, bonding, surface acidity, and morphology was performed by powder X-ray diffraction (XRD), $^{11}$B MAS NMR spectrometry, FT-IR spectrometry, pyridine-chemisorption IR spectrometry, and scanning electron microscopy (SEM). The composition of the prepared zeolites was determined by ICP-AES; the zeolite framework stability was investigated by steam treatment. The differences in the physicochemical properties of B-ZSM-5 prepared by the two methods were compared and discussed. In the direct synthesis, increasing initial boron-substitution ratio concomitantly brings about increasing difficulty to prepare pure B-ZSM-5 and, MFI-type borosilicate (free of aluminum) cannot be synthesized; the highest $SiO_2/Al_2O_3$ ratio = 70.64 is received. B-ZSM-5 prepared by the templating method shows remarkable hydrothermal stability than its counterpart prepared by the direct synthesis.


*Keywords:* B-ZSM-5; Direct synthesis; Templating method; MFI; Boroaluminosilicate; Borosilicate

## 1. Introduction

Microporous zeolites are crystallographically defined porous aluminosilicates that are classified as important solid catalyst or catalyst support. For the past four decades, ZSM-5 [1] has been a successful shape selective catalyst, particularly used in the petrochemical industry, coal industry, and fine chemical engineering. The $SiO_2/Al_2O_3$ ratio of ZSM-5 can be altered in a wide range for specific purposes, even to silica-based ZSM-5 (the silicalite-I), controlling its acid type, strength, and distribution. Isomorphous substitution for framework silicon and aluminum of the zeolites, either during the synthetic process or by a postsynthesis, is widely adopted since the introduced elements may bring about new physicochemical properties and catalytic performances by simultaneously preserving the zeolitic structural advantages. Many heteroatoms have been incorporated into the ZSM-5 framework, constructing the pentasil family with MFI zeotype. For instance, MFI-type titanosilicate (the TS-1) [2] is an efficient catalyst in the oxidation of many organics by hydrogen peroxide as well as under mild conditions. Another research work has documented MFI-type gallosilicate [3], Fe-MFI [4], Zn-ZSM-5 [5], etc.

Since Taramasso et al.'s first successful attempt [6] was made, a special focus has been fixed on the framework modification of ZSM-5 with boron; it is expected that MFI-type boroaluminosilicate and borosilicate possess gentle acidity and special catalytic capacities owing to partial or total replacement of framework aluminum, for instance in the Beckmann rearrangement [7]. Boroaluminosilicate with MFI zeotype (B-ZSM-5) is also considerable for preparing high $SiO_2/Al_2O_3$ ratio ZSM-5 since deboration is generally easier and more enhanced than dealumination. According to the literatures, the synthesis of B-ZSM-5 includes three preparative methods: (1) the hydrothermal synthesis: the preparation of zeolites under

*Corresponding author. Fax: +86 22 23509005.
*E-mail address:* sxliu@nankai.edu.cn (S. Liu).

0022-4596/$ - see front matter © 2005 Elsevier Inc. All rights reserved.
doi:10.1016/j.jssc.2005.12.013

hydrothermal conditions simulates their formation in natural surroundings; it is therefore the most frequently adopted method. Gabelica et al. [8] directly synthesized B-ZSM-5 in the Pyrex tube under highly alkaline conditions. Kessler et al. [9] prepared B-ZSM-5 in non-alkaline media of $NH_4F$ and $NH_4HF$, using tetrapropyl amine bromide (TPABr) as SDA, known as the "fluoride route". Brunner et al. [10] and Unger et al. [11] employed *n*-tripropylamine as SDA and boric acid as boron source to prepare B-MFI zeolite; (2) the wet impregnation: Sayed [12] received B-ZSM-5 by impregnating HZSM-5 in boric acid, and the product was characterized by spectroscopic methods of high resolution $^{11}B$ MAS NMR and IR; (3) the vapor phase method: Dong et al. [13] converted amorphous boron-containing aluminosilicate gel in the mixed gas atmosphere of $Et_3N$-EDA-$H_2O$ under a certain temperature and pressure. Some other articles fix concern on different perspectives, including the incorporation mechanism of boron and aluminum under hydrothermal conditions [14], thermal and chemical stabilities [15,16], and acid strength [15–17].

On the other hand, the synthesis of ZSM-5 generally requires solvated amine as structure-directing agent (SDA); the removal of SDA is carried out by subsequent calcination. The use of amine, however, may lead to high cost and environmental problems. Xiang et al. [18] successfully synthesized highly crystallized ZSM-5 without the employment of amine, which significantly reduced the industrial production cost. A new term "the direct synthesis" has been coined in the production of ZSM-5 ever since. However, it has been found to be difficult to prepare high $SiO_2/Al_2O_3$ ratio ZSM-5 in the direct synthesis, and efforts have been committed to increasing the $SiO_2/Al_2O_3$ ratio by a so-called "boration–deboration" strategy, that is, to replace as much as possible initial aluminum by boron in the direct synthesis, and afterwards, to wash boron off from the product by acid. By means of this boration–deboration route, Unger et al. [19] have promoted $SiO_2/Al_2O_3$ ratio to only 42. To what extent the $SiO_2/Al_2O_3$ ratio be promoted in direct synthesis through the boration–deboration route is one interest of this work.

So far, the direct synthesis of MFI-type boroaluminosilicate is very scarce due to the difficulty in synthesis. In the present work, B-ZSM-5 was synthesized by two methods under hydrothermal conditions. In the direct synthesis, commercial ZSM-5 (sodium form) was used as crystal seed, and in the templating method TPABr was employed as SDA. A series of physicochemical properties of B-ZSM-5 prepared by the two methods were compared and consequent differences were discussed, which lacking in previous researches and thus the concern of this paper.

## 2. Experiment

### 2.1. Materials

Water glass (industrial, $SiO_2 = 2.9069\,mol\,kg^{-1}$, $Na_2O = 0.8566\,mol\,kg^{-1}$, and $\rho = 1.2\,mol\,kg^{-1}$), aluminum sulfate (A.R.), and boric acid (A.R.) were employed as silicon, aluminum, and boron sources, respectively. Sulfuric acid (industrial, $2.8774\,mol\,kg^{-1}$, $\rho = 1.18\,mol\,kg^{-1}$) was used for the adjustment of the gel to requisite alkalinity. Ammonia chloride (A.R.) was employed in the ion exchange for receiving ZSM-5 of hydrogen form. All industrial materials were provided by the Chemical Plant of the Nankai University; they were directly used without any purification. Hydrogen chloride (A.R., $0.9\,mol\,L^{-1}$) was for deboration. Commercial ZSM-5 (sodium form, $SiO_2/Al_2O_3 = 38$, Catalyst Plant of Nankai University) acted as crystal seed. *N*-propylbromide (C.P.), *n*-tripropylamine (A.R.), and 2-butanone (A.R.) were chosen for the synthesis of TPABr. Sodium hydroxide (A.R., $6\,mol\,L^{-1}$) was used for dissolving zeolites in the ICP-AES and in the liquid $^{11}B$ NMR measurements.

### 2.2. Synthesis of structure-directing agent: TPABr

The synthesis of TPABr was as follows: equimolar *n*-propylbromide and *n*-tripropylamine were homogenously mixed in a Teflon-lined stainless-steel autoclave in the presence of 2-butanone as initiator. The autoclave was then sealed and placed under 373 K overnight. The resultant solid was recovered by filtration, washed with ether, and dried in the infrared radiation.

### 2.3. Synthesis of B-ZSM-5

#### 2.3.1. The direct synthesis

In the direct synthesis (hereafter DS), no amine was added as SDA. Aluminum sulfate, boric acid, and requisite sulfuric acid were dissolved in water; water glass was then added dropwise into the solution with vigorous stirring. Crystal seed (3 wt% of raw materials) was added into the gel, which was continuously stirred for maximum homogeneousness. The gel, with a molar composition of $5Na_2O{:}45SiO_2{:}(1-x)Al_2O_3{:}xB_2O_3{:}1840H_2O$, where $x$ is the boron-substitution ratio towards aluminum in the initial gel ($0 \leqslant x < 1$), was afterwards transferred into a Teflon-lined stainless-steel autoclave that was then sealed and kept under 453 K for 36 h. The resulting solid was recovered by filtration, washed with water until the filtrate was neutral, and finally dried. As-synthesized B-ZSM-5 prepared by DS is given the abbreviation of NaB-ZSM-5(DS).

#### 2.3.2. The templating method

In the templating method (hereafter TM), TPABr was first dissolved in water. Aluminum sulfate, boric acid, and water glass were added according to the molar ratio of oxides: $5Na_2O{:}45SiO_2{:}(1-x)Al_2O_3{:}xB_2O_3{:}1840H_2O{:}4.5$TPABr ($0 \leqslant x \leqslant 1$). Sulfuric acid was applied to adjust the pH value to the requisite alkalinity. The mixture gel proceeded with powerful stirring for homogeneousness, and was afterwards transferred into a Teflon-lined stainless-steel autoclave that was then sealed and kept under

453 K for 36 h. The resulting solid was recovered by filtration, washed with water until the neutral filtrate was received, and dried. The as-synthesized TPA-NaB-ZSM-5(TM) was finally calcined at 823 K for 5 h at a temperature-ramp of $1\,K\,min^{-1}$ and turned into NaB-ZSM-5(TM).

#### 2.3.3. Ion exchange

The ion exchange of NaB-ZSM-5 (sodium form) to HB-ZSM-5 (hydrogen form) is achieved by suspending 1 g zeolite in 10 mL ammonium chloride ($1\,mol\,L^{-1}$), and then heated at 363 K for 1 h. The solid, designated as $NH_4$B-ZSM-5, was filtrated out and washed with water. The exchange procedure was repeated three times for enhanced exchange level. The resulting solid was calcined at 723 K for 5 h at a temperature-ramp of $1\,K\,min^{-1}$. The calcined sample is designated as HB-ZSM-5.

## 3. Characterization

### 3.1. Powder X-ray diffraction (XRD)

Powder XRD data were collected on a Rigaku D/max-RAX diffractometer with monochromatic Cu$K\alpha$ radiation ($\lambda = 0.154$ nm) operated under 40 kV and 100 mA. The $2\theta$ value was scanned in the range of 5–35° with a resolution of $2^\circ\,min^{-1}$. In the present paper, the content of the relevant phase is relatively represented by the integral of the corresponding diffraction peaks.

### 3.2. Nuclear magnetic resonance spectrometry (NMR)

Solid state NMR is a common method for determining the incorporated heteroatoms in the zeolite configuration. $^{11}$B MAS NMR spectra were acquired on a Varian UNITY-Plus 400 Fourier Transform NMR spectrometer at the $^{11}$B resonance frequency of 128.359 MHz. Magic angle spinning was set to 7.5 kHz. $BF_3 \cdot OEt_2$ was employed as a reference to the chemical shift. In the liquid $^{11}$B NMR measurement for analyzing the framework boron content, $^{11}$B NMR spectra in $D_2O$ were obtained on a Varian Mercury Vx300 Fourier Transform NMR spectrometer at the $^{11}$B resonance frequency of 96.278 MHz.

### 3.3. Fourier transform infrared spectrometry (FT-IR)

FT-IR was operated on a Bruker VECTOR22 Fourier Transform infrared spectrometer in the mid-infrared range of 400–4000 $cm^{-1}$. It was conducted using KBr wafers (1 wt% sample mixed with 99 wt% KBr). The Lewis/Brönsted acid ratio of HB-ZSM-5 was evaluated by the pyridine-chemisorption FT-IR spectrometry on self-supported wafers.

### 3.4. Induction-coupled plasma atomic emission spectroscopy (ICP-AES)

ICP-AES measurement was carried out by an IRIS Advantage ICAP full spectrum direct-reading emission spectrometer manufactured by TJA Solutions (US). About 0.05 g of the sample was quantified and completely dissolved by 30 mL sodium hydroxide ($6\,mol\,L^{-1}$) in a Teflon-lined stainless-steel autoclave that was sealed and placed in a 453 K atmosphere overnight. Then, the homogenous solution was diluted with great accuracy in volume. The concentrations of framework silicon, aluminum, and boron were determined.

### 3.5. Scanning electron microscopy (SEM)

Crystal morphology and outline were observed on a Hitachi S3500 microscope. Gold was insufflated onto the sample as electric media.

## 4. Results and discussion

### 4.1. Characterization of B-ZSM-5

#### 4.1.1. Powder X-ray diffraction

The XRD patterns of NaB-ZSM-5(DS0.5) and TPA-NaB-ZSM-5(TM0.5) (the suffix "0.5" is the $x$ value) are shown in Fig. 1A ((a) and (b), respectively). The XRD patterns reveal specific diffraction of MFI-type zeolite structure, which is mainly reflected in the peaks located at around $2\theta = 7$–10° with three reflections, in around 23–25° range with five reflections, and at around 29–30° with three reflections. (The sum integral of peak from the three regions is assigned to the MFI phase.) The jutting projection observed in the $2\theta = 25$–27.5° range of NaB-ZSM-5(DS0.5), compared with TPA-NaB-ZSM-5(TM0.5) in this region, arises from the impurity of compact silicate (nonporous) formed by excess silicon due to lack of aluminum in the DS. In both synthetic cases we have tried to increase the $x$ value, and, thus, to promote the $SiO_2/Al_2O_3$ ratio by employing boron for the substitution of initial aluminum. In DS, the compact silicate as an impurity evidently appeared to be unavoidable when $x$ was exceeded beyond 0.5; it was also increased along with the increased content of boron in the initial gel and grew larger overall from 25 to 27.5° as can be observed in the XRD patterns (Fig. 1B). Also, in the DS, an effort to prepare MFI-type borosilicate was futile ($x = 1$); actually, under present experiment conditions, when $x$ was 0.8, a large and intense X-ray diffraction overall due to compact silicate was observed, indicating the impurity of the MFI phase; when $x$ was 0.85 or higher, the synthesized sample contained no MFI phase shown by XRD. It could be therefore concluded that MFI-type borosilicate cannot be received without the employment of SDA. In the DS, higher substituted boron content in initial gel increases the difficulty, making it even impossibe to prepare pure

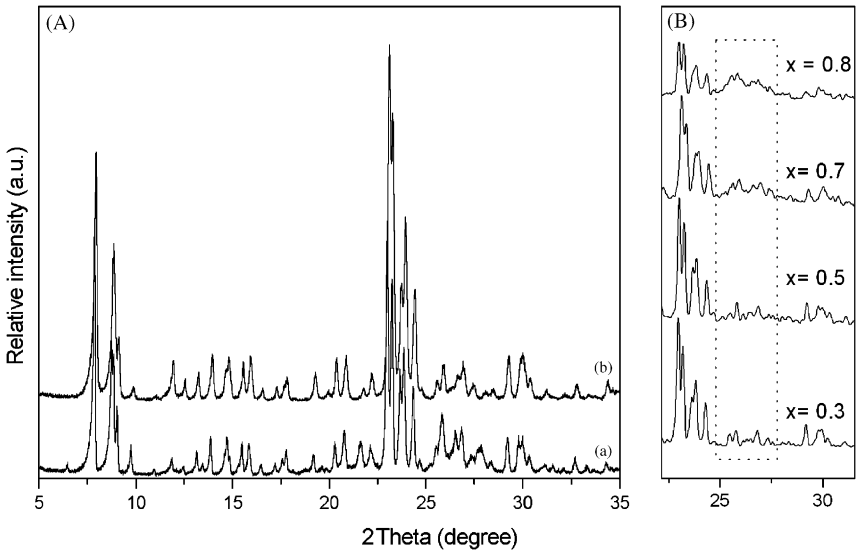


Fig. 1. A: XRD patterns of (a) NaB-ZSM-5(DS0.5) and (b) TPA-NaB-ZSM-5(TM0.5); B: partial XRD patterns of NaB-ZSM-5(DS), a growing projection juts out along with increasing $x$ value.

B-ZSM-5. In contrast, in the TM, arbitrary boron-substitution ratio ($0 \leqslant x \leqslant 1$) can be chosen for synthesizing highly crystallized B-ZSM-5, even for aluminum-free borosilicate with MFI zeotype, promoting $SiO_2/Al_2O_3$ ratio to the limited degree. NaB-ZSM-5(TM) maintains the remarkable purity of MFI phase; no obvious compact silicate species can be observed in the XRD patterns of NaB-ZSM-5(TM).

#### 4.1.2. $^{11}B$ MAS NMR spectrometry

The existence of four-coordinated boron in the zeolite framework is evidenced by the observation of a sharp resonance peak located at around $-3$ ppm from $BF_3 \cdot OEt_2$ in the spectrum (Fig. 2) [20]. This resonance disappears when deboration by hydrogen chloride is carried out (figure not shown), indicating boron was washed off from the framework. Deboration was carried out by suspending NaB-ZSM-5 in refluxing hydrogen chloride three times with a time length of 1 h each. $^{11}B$ MAS NMR suggests that boron could be successfully incorporated into the zeolite framework in the form of $BO_4$ tetrahedron with the formation of B–O–Si bond by the DS. No other existent types of boron are detected by $^{11}B$ MAS NMR in the NaB-ZSM-5(DS). NaB-ZSM-5(TM) shows similar $^{11}B$ MAS NMR spectra (not shown).

#### 4.1.3. Fourier transform infrared spectrometry

The IR spectra of NaB-ZSM-5(DS0.5) and TPA-NaB-ZSM-5(TM0.5) are given in Fig. 3. The IR peak at around 668 $cm^{-1}$ is assigned to the symmetric bending vibriation of Si–O–B bond [21]. The peak at around 913 $cm^{-1}$ is documented in a previous work [21], which could be observed in all of the boron-contained zeolites, characteristic of symmetric stretching vibration of Si–O–B bond. The IR spectra also evidence the existence of boron in the

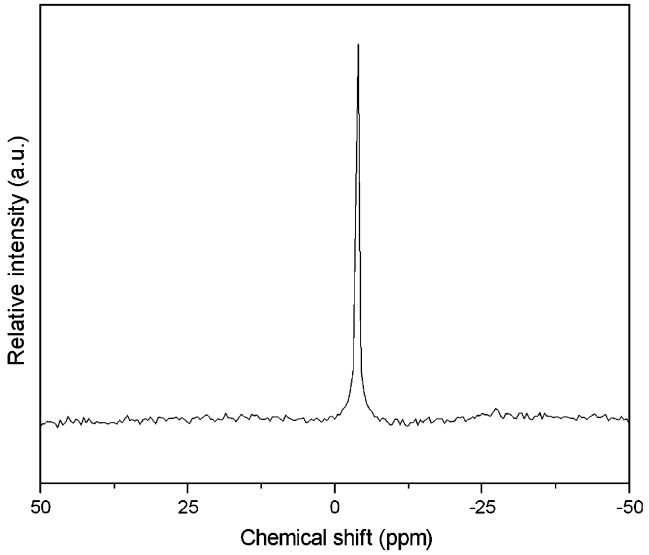


Fig. 2. $^{11}B$ MAS NMR spectrum of NaB-ZSM-5(DS0.5)

B-ZSM-5 framework. Besides, the vibrational band at 547 $cm^{-1}$ confirms the presence of a five-membered ring of the pentasil structure; the wide and intense Si–O–Si stretching band in the saturated region from 1000 to 1300 $cm^{-1}$ due to $SiO_2$ tetrahedron of NaB-ZSM-5(DS0.5) shows a little distortion (indicated with arrows in the spectrum), which may be due to the framework defect that will be discussed later. The weak peak at 1385 $cm^{-1}$ is assigned to tri-coordinated framework boron [22], which is out of the detection limit of $^{11}B$ MAS NMR.

The pyridine-chemisorption IR spectra of HB-ZSM-5(DS0.5) and HB-ZSM-5(TM0.5) are shown in Fig. 4. The peak at 1545 $cm^{-1}$ indicates the interaction of pyridine rings with the Brönsted acid sites, the peak at 1446 $cm^{-1}$

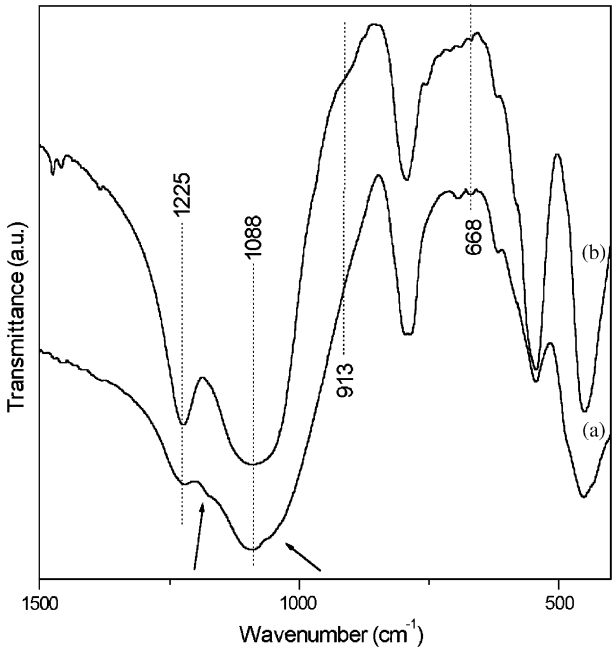


Fig. 3. FT-IR spectra of (a) NaB-ZSM-5(DS0.5) and (b) TPA-NaB-ZSM-5(TM0.5).

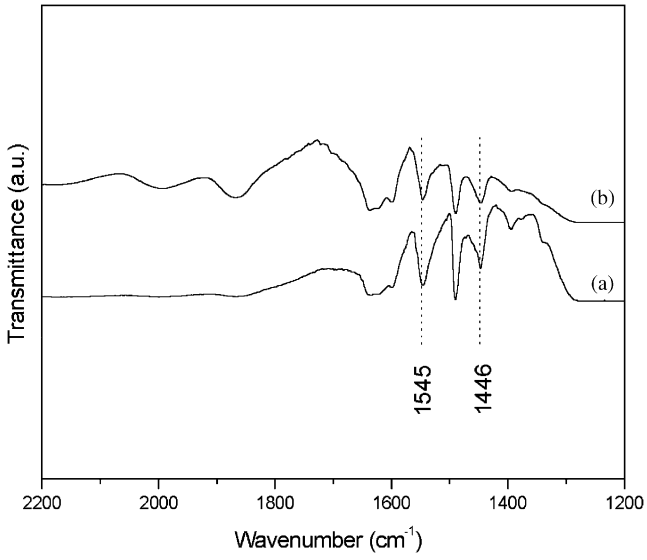


Fig. 4. Pyridine-chemisorption IR spectra of (a) HB-ZSM-5(DS0.5) and (b) HB-ZSM-5(TM0.5).

indicating the interaction with Lewis acid sites [15]. A Lewis/Brönsted acid ratio (integral of relevant peak) of 0.42 was received on the HB-ZSM-5(DS0.5) sample, and 0.79 on the HB-ZSM-5(TM0.5) sample. Pyridine-chemisorption IR spectra suggest HB-ZSM-5(TM0.5) has more Lewis acid sites than Brönsted site, which may be due to tri-coordinated boron generated during the calcination [23].

#### 4.1.4. Scanning electron microscopy

SEM micrographs (Fig. 5) reveal that both synthesis yield spindle-type crystals of B-ZSM-5. As is observed in the SEM micrographs, NaB-ZSM-5(DS0.5) crystals are dimensionally larger than TPA-NaB-ZSM-5(TM0.5) and are also slightly agglomerate. This is because the use of template generally results in small zeolite crystals. In contrast, in the DS, crystals may grow larger with the nuclei of crystal seeds. In both cases, crystals are not uniform in crystal size distribution on account of the static crystallization process.

#### 4.1.5. Crystal seed and the template

B-ZSM-5(0.5) was synthesized for a comparison by both methods. The growth of MFI and heterophase is recorded and plotted in Fig. 6. When crystallization time was 8 h under present experiment conditions, both cases showed amorphous silica. As is clearly shown in the Fig. 6, the crystal seed accelerated the growth of MFI phase, and in the meantime, the heterophase of compact silicate grew rapidly. When crystallization time was prolonged to 36 h, the MFI phase gradually converted into compact silicate (aluminum staying in liquid). In contrast, the MFI phase gradually formed when TPABr was in existence as an SDA that helped the zeolite maintain its specific structure since the compact silicate grew at a significant low level. It could be also concluded from Fig. 6 that in the DS, compact silicate may form not only from excess silicon due to lack of aluminum, but also by the conversion of MFI phase due to exceeded crystallization time.

The framework boron content is different by the two methods. $BO_4$ tetrahedron is much smaller than $AlO_4$ tetrahedron since boron is smaller than aluminum in atomic radius. According to the Coulomb's Law, the electrostatic force between two charges is in inverse square ratio with the distance between them. Therefore, the interaction between $BO_4^-$ and $TPA^+$ is more intense than $AlO_4^-$ with the large SDA cation. Under the attraction of the SDA TPABr, in comparison with the case of the DS, boron has more opportunity to be located in the zeolite framework in the templating situation. Fig. 7 shows that in the TM for synthesizing B-ZSM-5, compared with the DS, lower Si/B ratio and higher Si/Al ratio are received, which is in agreement with the above statement.

#### 4.1.6. Different boron contents

NaB-ZSM-5 prepared by the two approaches, the DS and the TM, were determined of silicon, aluminum, and boron contents by the ICP-AES. In Fig. 7, the dot lines are relevant ratios in initial gels, with the terminals located at limited positions since one of the components (Al or B) is not added. The real lines stand for the relevant ratios, Si/Al or Si/B, which are acquired by ICP-AES. It is noticeable in the DS that the Si/B ratio when $x = 0.7$ is higher than that when $x = 0.5$, indicating less boron content. When the ratio of boron added in the initial gel is exceeded beyond 50%, the heterophase compact silicate is of unavoidable existence as is shown by XRD. The compact silicate is composed of excess silicon, forming a solid that mixes with B-ZSM-5(DS) in the product. On the contrary, excess

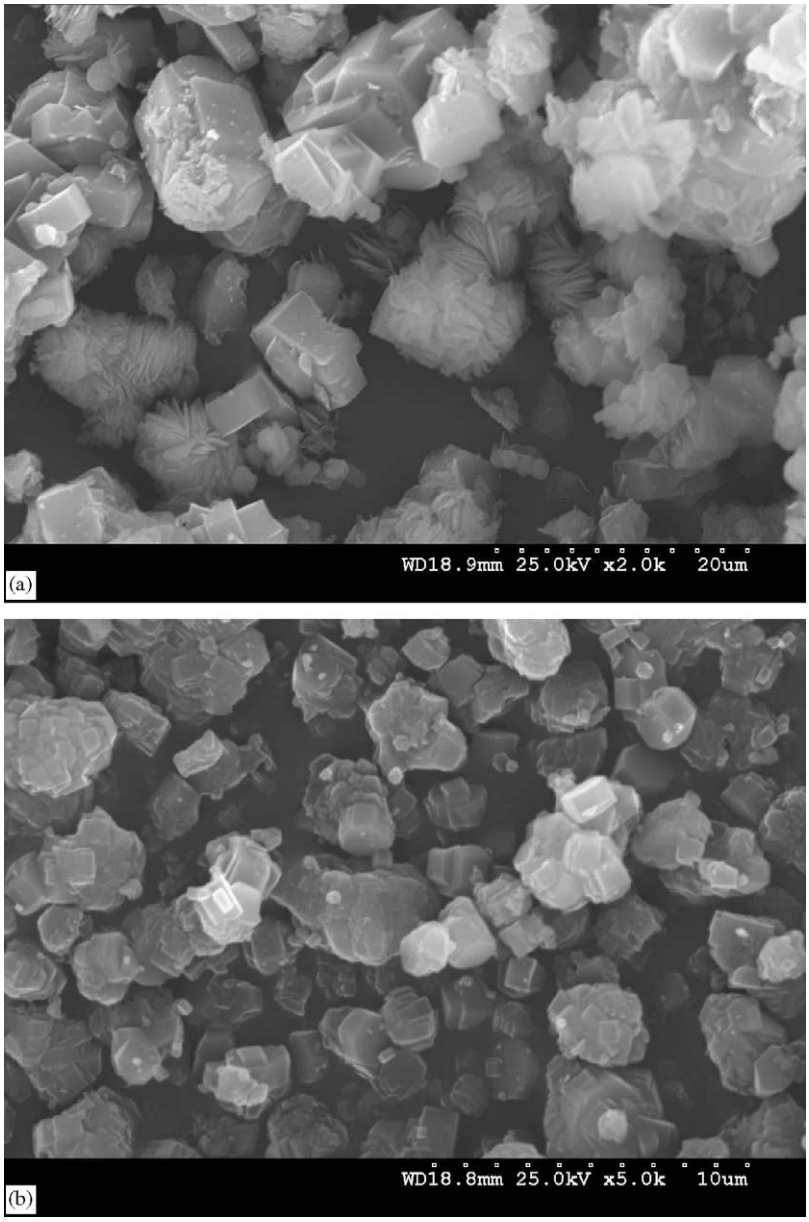


Fig. 5. SEM micrographs of (a) NaB-ZSM-5(DS0.5) and (b) TPA-NaB-ZSM-5(TM0.5).

boron will remain in the liquid phase. ICP-AES gives data for solid product, of boron content only in MFI phase and silicon content in both MFI and compact silicate, or rather the "solid phase". When boron in initial gel is more than a half, excess boron would be neither incorporated into the MFI framework nor into the heterophase, resulting in increased Si/B ratio. The Si/Al ratio alternates with the theoretical line all along. In other words, for B-ZSM-5(DS), framework boron tends to a limit when $x = 0.5$; excessive adding of boron will no longer decrease Si/B ratio. In order to verify this, B-ZSM-5(DS) samples with $x = 0.2$, 0.3, 0.5, and 0.7 were accurately quantified in 0.5000 g, dissolved by 5 mL sodium hydroxide (6 mol $L^{-1}$), and measured in $^{11}B$ liquid NMR experiment. A curve is plotted in Fig. 8 with the purpose of determining the boron content. A peak also occurs on the boron-substitution axis at $x = 0.5$. Therefore in the DS, excessive substituted boron added beyond half will not help increase framework boron content; the MFI, however, would be decreased with increased boron since relatively excess silicon would form compact silicate. On the other hand, Si/B ratio decreases all along, indicating increasing boron content in B-ZSM-5(TM) samples. In DS, when initial gel composition was $45SiO_2{:}0.8B_2O_3{:}0.2Al_2O_3$, a highest $SiO_2/Al_2O_3$ ratio of NaB-ZSM-5(DS) = 70.64 was determined by ICP-AES.

Dynamic crystallization (the gel was continuously stirred during the crystallization) was adopted in the DS. The crystallization time for well-crystallized B-ZSM-5 (the standard was well-resolved, XRD pattern acquired, and

most purity observed in SEM micrograph) is recorded and plotted in Fig. 9. Such crystallization time decreases with the increase of boron in initial gel, implying the accelerated crystallization. This might be attributed to the very weak acidity of boric acid though on which we used to expect neutralization with alkali in the gel, resulting in the decreased sulfuric acid added. B-ZSM-5(DS) consequently grows faster under actually increased alkalinity. Also in Fig. 9, the dot line is plotted according to the MFI phase content calculated from the prepared samples received at each of the recommended crystallization time (the real line in the figure). It shows a gradual decrease in the MFI content along with increased boron-substitution ratio, owing to the dissolution of silicon, aluminum, and boron under higher alkalinity.

### 4.2. Steam treatment

The hydrothermal stability of B-ZSM-5(0.5) prepared by the two methods was evaluated by the steam treatment. The sample was shallow-bed stored in a porcelain container, which was located in a tube cooker. Steam speed was carefully controlled at 2.2 mL $min^{-1}$. The steam treatment lasted for 4 h at different temperatures. The treated samples were characterized by powder XRD, with the relative crystallinity curves plotted in Fig. 9. As is clearly shown in the figure, B-ZSM-5(TM0.5) is hydrothermally more stable than the DS-prepared counterpart. The crystallinity of B-ZSM-5(DS0.5) evidently decreased when process temperature was higher than 673 K; at 878 K, MFI phase and α-$SiO_2$ can both be observed in the XRD pattern (now shown); at 973 K, B-ZSM-5(DS0.5) completely converted

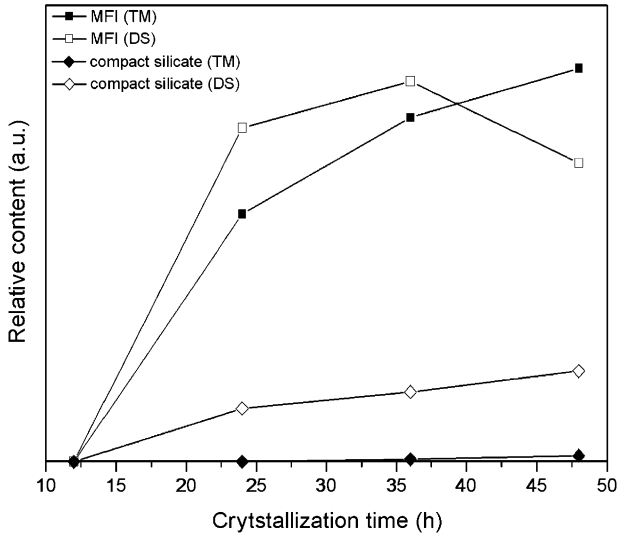


Fig. 6. The growth of MFI phase and impurity compact silicate phase ($x = 0.5$).

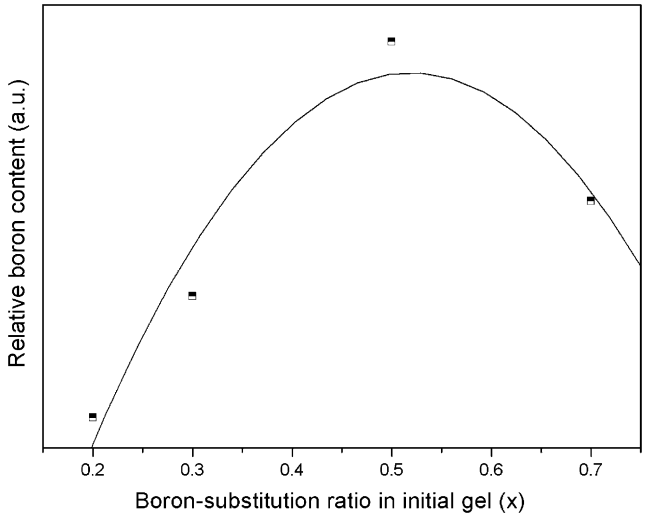


Fig. 8. Relative boron content of NaB-ZSM-5(DS) determined by liquid $^{11}B$ NMR spectrometry.

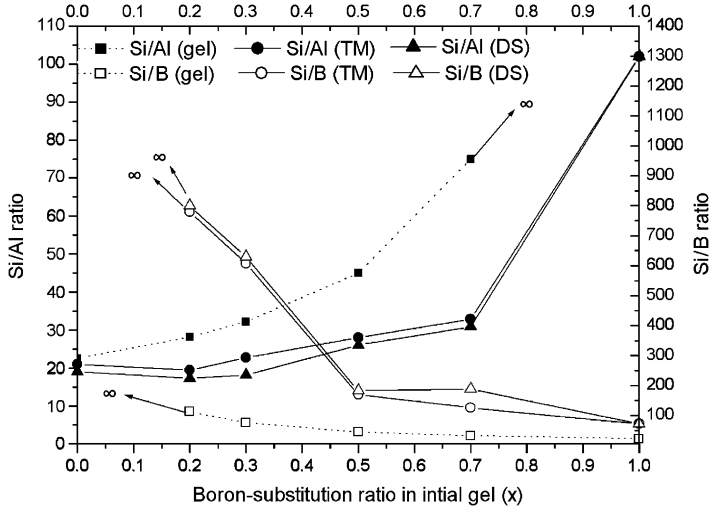


Fig. 7. Relevant Si/Al ratio and Si/B ratio towards initial boron-substitution ratio.

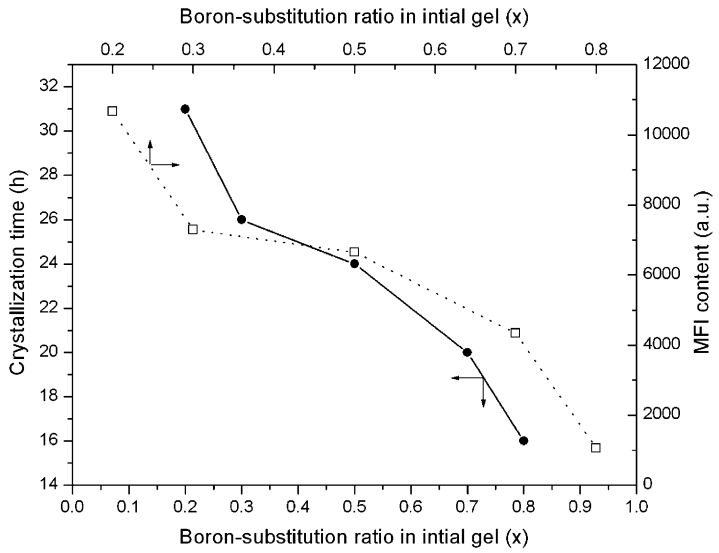


Fig. 9. Crystallization time for receiving well-crystallized NaB-ZSM-5(DS) with different boron-substitution ratios in the initial gel (real line) and the corresponding MFI content (dot line).

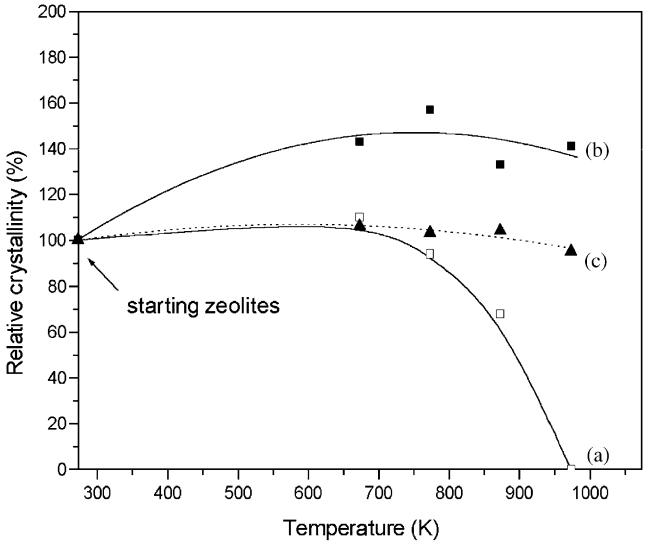


Fig. 10. Relative crystallinity of (a) NaB-ZSM-5(DS0.5), (b) NaB-ZSM-5(TM0.5), and (c) Al-ZSM-5(DS0) after the steam treatment.

into α-$SiO_2$. In contrast, B-ZSM-5(TM0.5) maintained remarkable, typical MFI structure even when treated at higher temperatures, with no obvious decrease in crystallinity or collapse of framework occurring (Fig. 10(b)).

The boron-free Al-ZSM-5(DS0) prepared by the DS maintains its specific MFI structure through the steam treatment (the dot line in Fig. 10(c)) that indicates the methodology, the DS itself, is not the reason that should account for the instability of B-ZSM-5(DS0.5) towards present hydrothermal conditions, while B-ZSM-5(TM0.5) is also hydrothermally stable under the same treatment conditions, implying that framework heteroatom boron is not the reason either. Therefore, it is concluded the main feature that causes the hydrothermal instability of B-ZSM-5(DS) is the defect that distorts the Si–O–Si stretching, as is observed in the IR spectrum (Fig. 3(a)), occurs in the zeolite framework. Although many researches have successfully incorporated heteroatoms into the MFI framework, yet from the crystallography point of view, only silicon and aluminum theoretically match a tetrahedron configuration with four oxygen atoms in the vertices and a T-atom located in the center on account of the atomic radii. ICP-AES determines that the framework boron is rather limited owing to its unsuitability in the $BO_4$ construction; in the DS, the initial boron may experience a reversible process from the zeolite framework to the liquid phase without the stabilization of the template $TPA^+$, forming an equilibrium from solid to liquid, leaving much defect in the framework that causes the distortion of Si–O–Si stretching, and leading to the resultant behavior in the steam treatment. On the contrary, the adopted amine as SDA restrains from the pealing off of the framework boron, stabilizing its framework. Therefore, the affection of heteroatom boron during the hydrothermal DS should be enhanced along with the increased boron-substitution ratio ($x$) in the initial gel. It might be verified by the enriched initial boron in the DS. Steam treatment was then carried out on different direct-synthesized samples with different $x$'s. In Fig. 11, the samples with $x = 0.2$ and 0.3 maintains, though somewhat less regular due to the local collapse of the framework, the MFI structure after being treated at 973 K. At this temperature, both samples with $x = 0.5$ and 0.7 convert completely into α-$SiO_2$. All samples reveal a critical turning point at around 773 K; the increase in crystallinity at the beginning of the treatment may be due to continued crystallization and re-regularization under hydrothermal treatment conditions [25].

Fig. 12 gives the IR spectra of B-ZSM-5(DS0.5) treated at different temperatures. The peak at 668 $cm^{-1}$ assigned to the symmetric bending of Si–O–B bond in $BO_4$ configuration disappears in the treated samples, indicating the rupture of O–B bond after the hydrothermal treatment. Also, the intensity of the IR peak at about 3665 $cm^{-1}$ appointed to the bridging hydroxyl Si–OH–Al(or B) is decreased with the rise of treat temperature; a new peak at around 3740 $cm^{-1}$, assigned to the Si–OH in silanol nests [24], is increased in intensity, which may be attributed to the dealumination [26] and deboration as well as the formation of α-$SiO_2$. Meanwhile, the adsorption peak at around 550 $cm^{-1}$ appointed to the MFI zeotype gradually decreases in intensity and finally disappears, indicating the conversion of pentasil zeolite. For the B-ZSM-5(TM0.5), there is no obvious observation of the change in the typical MFI zeotype framework (Fig. 13). Dealumination/deboration can also be confirmed since the adsorption peak at around 3665 $cm^{-1}$ appointing to the Si–OH–Al(B) also weakens with the rise the treat temperature. The difference lies in that B-ZSM-5(TM0.5) preserves some Si–OH–Al(B) sites to a remarkable extent since the peak at 3665 $cm^{-1}$ is clear after steam treatment at 973 K , implying the stability of the framework.

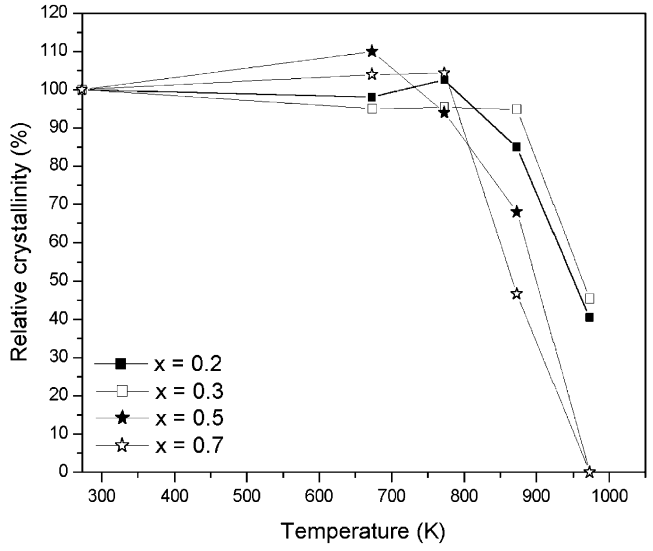


Fig. 11. Relative crystallinity of NaB-ZSM-5(DS) with different boron-substitution ratios after the steam treatment.

## 5. Conclusions

Boron-incorporated MFI-type boroaluminosilicate (B-ZSM-5) can be successfully synthesized by the DS in which sodium form ZSM-5 ($SiO_2/Al_2O_3 = 38$) is used as crystal seed, and the TM by the employment of TPABr as the structure-directing agent. MFI-type borosilicate (free of aluminum) can only be prepared when the amine is used. In the DS, higher substituted boron towards aluminum would increase the difficulty, making it even impossibe to prepare pure MFI-type B-ZSM-5, resulting in the increasing impurity of compact silicate. Relevant characterization of powder XRD, $^{11}B$ MAS NMR, FT-IR, and SEM demonstrated the specific structure of MFI-type zeolite as

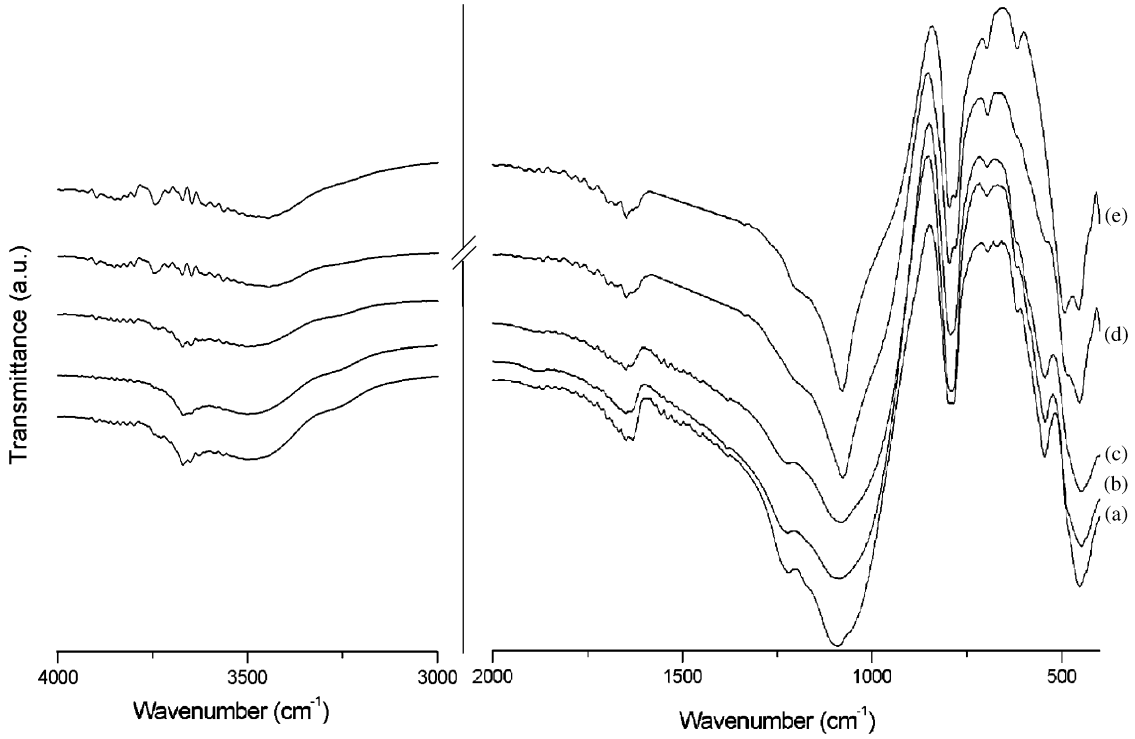


Fig. 12. FT-IR spectra of (a) NaB-ZSM-5(DS0.5), NaB-ZSM-5(DS0.5) steam-treated (b) at 673 K, (c) at 773 K, (d) at 873 K, and (e) at 973 K.

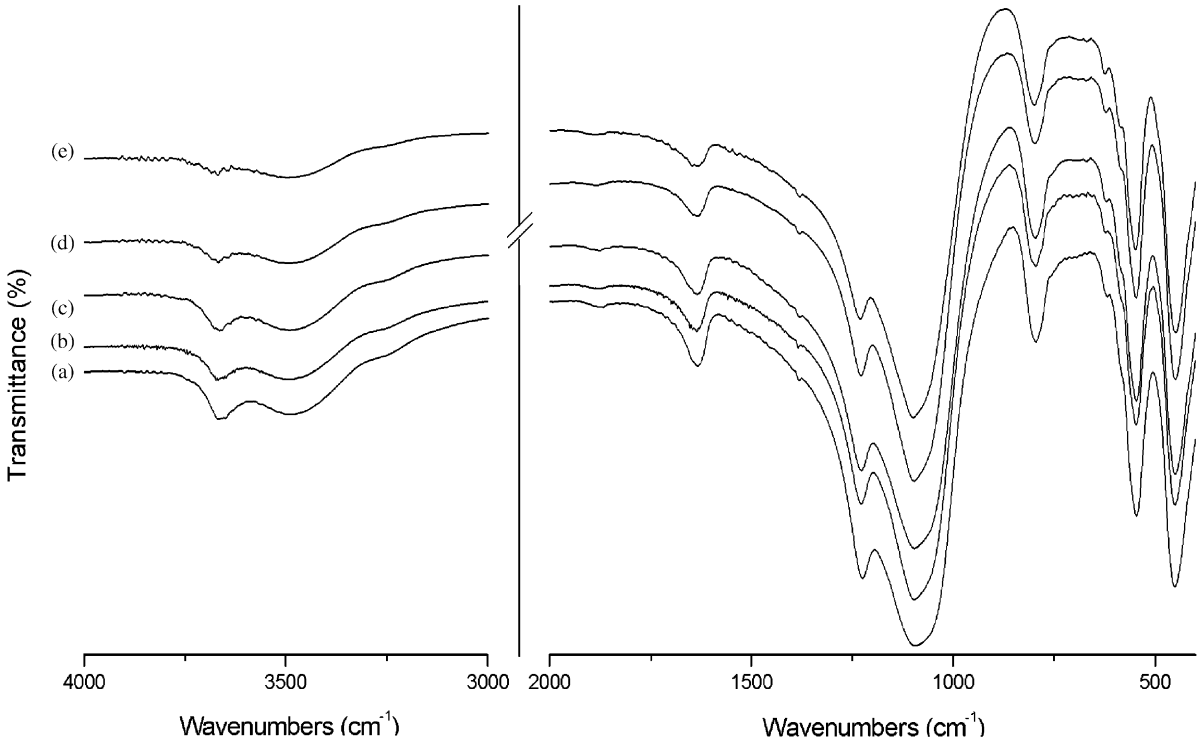


Fig. 13. FT-IR spectra of (a) NaB-ZSM-5(TM0.5), NaB-ZSM-5(TM0.5) steam-treated (b) at 673 K, (c) at 773 K, (d) at 873 K, and (e) at 973 K.

well as the existence of four-coordinated boron in the framework through the two approaches.

Crystal seed and SDA play quite different roles in the formation of B-ZSM-5 zeolites. Crystal seed speeds up the growth of MFI phase, but without restraining the occurrence of heterophase compact silicate, which is significantly unavoidable when boron-substitution ratio in initial gel is beyond a half. Although in the TM the MFI phase grows significantly slowly, the purity of the requisite MFI phase is satisfying. Meanwhile, in case that tri-covalent species aluminum and boron are both existent in the synthetic system, boron has more opportunity to be incorporated in to the framework under the attraction of template cation in the TM than in the DS.

Existent boron in the B-ZSM-5 framework is found to be rather limited due to its unsuitability in the zeolitic $TO_4$ construction. In the DS, framework boron arrives at a maximum when initial substituted boron ratio is 0.5. Excess of added boron would stay in the liquid. The DS yields the highest $SiO_2/Al_2O_3$ ratio of 70.64.

B-ZSM-5 synthesized by the TM shows more remarkable hydrothermal stability than the counterpart by the DS.

## Acknowledgments

This work is financially supported by the National Science Foundation of China (Grants 29973016 and 20233030), and the Ministry of Education of China.

## References

[1] (a) US Patent, 3702866 (1972).;
(b) G.T. Kokotailo, S.L. Lawton, D.H. Olson, W.M. Meier, Nature 272 (1978) 437.
[2] US Patent, 4410501 (1983).
[3] R. Fricke, H. Kosslick, G. Lischke, M. Richter, Chem. Rev. 100 (2000) 2303.
[4] R. Szostak, T.L. Thomas, J. Catal. 100 (1986) 555.
[5] J. Liang, W. Tang, M.L. Ying, S.Q. Zhao, B.Q. Xu, H.Y. Li, Studies in Surface Science and Catalysis, Elsevier, Amsterdam, 1991.
[6] M. Taramasso, G. Perego, B. Notari, in: L. V. Rees (Ed.), Proceedings of the fifth International Conference on Zeolites, Heyden & Son, London, 1980, p. 40.
[7] J. Röseler, G. Heitmann, W.F. Hölderich, Appl. Catal. A: Gen. 144 (1996) 319.
[8] Z. Gabelica, J.B. Nagy, P. Bodart, et al., Chem. Lett. 151 (1984) 1059.
[9] H. Kessler, J.M. Chezeau, J.L. Guth, H. Strub, G. Coudurier, Zeolites 7 (1987) 360.
[10] E. Brunner, D. Freude, M. Hunger, H. Pfeifer, W. Reschetilowski, B. Unger, Chem. Phys. Lett. 148 (1988) 226.
[11] B. Unger, K.P. Wendlandt, H. Toufar, W. Schwieger, K.H. Bergk, E. Brunner, W. Reschetilowski, J. Chem. Soc. Faraday Trans. 87 (1991) 3099.
[12] M.B. Sayed, J. Chem. Soc. Faraday Trans. 83 (1987) 1751.
[13] J.X. Dong, X.G. Zhao, F. Zhou, Chin. J. Inorg. Chem. 11 (1995) 73.
[14] R. de Ruiter, J.C. Jansen, H. van Bekkum, Zeolites 12 (1992) 56.
[15] M.W. Simon, S.S. Nam, W.-Q. Xu, S.L. Suib, J.C. Edwards, C.-L. O'young, J. Phys. Chem. 15 (1992) 6381.
[16] C.T.-W. Chu, C.D. Chang, J. Phys. Chem. 89 (1985) 1569.
[17] M.G. Howden, Zeolites 5 (1985) 334.
[18] (a) H. Li, S. Xiang, D. Wu, Y. Liu, X. Zhang, S. Liu, Chem. J. Chinese U. 4 (1981) 517
(b) PRC Patent, 85100463 (1988).

[19] B. Unger, K.-P. Wendlandt, H. Toufar, W. Schwieger, K.-H. Bergk, E. Brunner, W. Reschetilowski, J. Chem. Soc. Faraday Trans. 87 (1991) 3099.
[20] B. Sulikowski, J. Klinowski, J. Phys. Chem. 96 (1992) 5030.
[21] M.A. Camblor, A. Corma, J.P. Pariente, J. Chem. Soc., Chem. Commun. 7 (1992) 360.
[22] M.B. Sayed, A. Auroux, J. Vedrine, J. Catal. 116 (1989) 1.
[23] R. de Ruiter, A.P.M. Kentgens, J. Grootendorst, J.C. Jansen, H. van Bekkum, Zeolites 13 (1993) 128.
[24] M. Selvarej, A. Pandurangan, K.S. Seshadri, Appl. Catal. A: Gen. 242 (2003) 347.
[25] R.M. Barrer, M.B. Makki, Can. J. Chem. 66 (1964) 1366.
[26] B. Kraushaar, J.H.C. van Hooff, Catal. Lett. 1 (1988) 81.